Available online at www.sciencedirect.com
SCIENCE DIRECT
Journal of Chromatography B, 826 (2005) 177–187
JOURNAL OF CHROMATOGRAPHY B
www.elsevier.com/locate/chromb

A platform for high-throughput molecular characterization of recombinant monoclonal antibodies

Mark J. Bailey [a], Andrew D. Hooker [b,1], Carolyn S. Adams [c], Shuhong Zhang [c], David C. James [a,*]

[a] *School of Engineering, University of Queensland, St. Lucia, Qld 4072, Australia*
[b] *Pfizer Analytical Research and Development, Sittingbourne, Kent ME9 8AG, UK*
[c] *Pfizer Global Research and Development, St. Louis, MO, USA*

Received 18 February 2005; accepted 31 August 2005
Available online 19 September 2005

Abstract

We describe quantitative characterization of a sample preparation platform for rapid and high-throughput analysis of recombinant monoclonal antibodies (MAbs) and their post-translational modifications. MAb capture, desalting and in situ reduction/alkylation were accomplished by sequential adsorption of analyte to solid phase beads (protein A, reverse-phase) suspended in microtiter plate wells. Following elution and rapid tryptic digestion in the presence of acid-labile surfactant (RapiGest™), peptides were fractionated by stepwise elution from reverse-phase pipet tips and the fraction containing Fc *N*-glycopeptides isolated. Direct quantitative analysis of the relative abundance of peptide glycoforms by MALDI-TOF MS in linear mode closely correlated with normal phase HPLC analysis of fluorophore labeled *N*-glycans released by PNGaseF.

Keywords: IgG2; Recombinant monoclonal antibody; Glycosylation; Glycopeptide; High-throughput characterization; Normal phase liquid chromatography; MALDI-TOF MS

1. Introduction

Molecular heterogeneity of recombinant monoclonal antibodies (MAbs) is an important issue for the biopharmaceutical industry; potentially affecting product definition, consistency, potency and purity. Consequently, rigorous analytical characterization is necessary to satisfy the requirements of regulatory agencies [1].

MAbs are hetero-tetrameric proteins consisting of two heavy chains (or gamma chains in the case of IgGs) and two light (kappa or lambda) chains. Heterogeneity may derive from variation in primary amino acid sequence, stoichiometry of heavy and light chains, aggregation of the antibody product or a variety of post-translational modifications such as proteolytic cleavage, oxidation and/or deamidation reactions and variable *N*-glycosylation. The latter is crucial, for example, in the case of recombinant MAbs which are designed to harness biological activities such as antibody dependent cell cytotoxicity and complement mediated lysis in vivo [2,3]. Molecular heterogeneity may arise from a variety of sources. For example, for MAbs produced by mammalian cells in culture, the expression system may itself define *N*-glycan processing [4,5], and variations in cell culture conditions can also affect MAb post-translational modifications [6–11].

While advances in a variety of techniques now permit very detailed assessment of recombinant protein primary structure and post-translational modifications off-line (e.g. MS, LC, CE), the inherent structural diversity of recombinant proteins requires each product to be treated as a unique analytical challenge. The development of analytical procedures (as a necessary prerequisite for effective bioprocess development) is often a bottleneck to progress.

Monoclonal antibodies (despite subclass specific variation) are a structurally homogeneous group which should be amenable to the development of generic sample processing and analytical approaches. Despite this, there are few examples of integrated strategies for MAb analysis [12,13]. Aside from speeding the

* Corresponding author. Tel.: +61 7 3365 4638; fax: +61 7 3365 4199.
E-mail address: davidj@cheque.uq.edu.au (D.C. James).
[1] Present address: Pharmaceutical Sciences, Celltech 216 Bath Road, Slough SL1 4EN, UK.

1570-0232/$ – see front matter © 2005 Elsevier B.V. All rights reserved.
doi:10.1016/j.jchromb.2005.08.021

Table 1
Microplate-based sample processing strategy for high-throughput monoclonal antibody characterization

Process step	Cumulative process time (h)	Sample input	Sample preparation (separation/process)	Analyte output[a]	Possible orthogonal analyses[b]	
					Analysis	Method
1 MAb capture/purification	1	Clarified culture supernatant	Affinity capture on rProtein A Sepharose resin, washing and elution	Pure MAb in 100 mM Tris, 45 mM glycine	MAb quantitation	Microplate spectrometry
					MAb aggregation	GFC [14]
					MAb half antibody (non-disulfide bonded heavy chain)	NR SDS-PAGE [15–17]
					MAb charge variants	IEX [18–20]
						CE [21,22]
2 Desalting and/or reduction and alkylation	2–4	Pure MAb in 100 mM Tris, 45 mM glycine	Immobilization on reverse phase resin, desalting and/or reduction and alkylation and elution	Pure MAb or reduced and alkylated MAb in 50% CH_3CN/0.1% TFA	Mass analysis of whole MAb or reduced and alkylated heavy and light chains	MALDI-TOF MS [12,23,24]
					Separation of reduced and alkylated heavy and light chains for separate analysis	RP-HPLC [25]
3 Sample drying and enzymatic digestion	4–6	Pure MAb or reduced and alkylated MAb in 50% CH_3CN/0.1% TFA	Vacuum assisted drying and trypsin digestion in RapiGest	Tryptic peptides in 50 mM ammonium bicarbonate containing 0.5% RapiGest	Peptide mapping (reduced and alkylated MAb digest only)	MALDI-TOF MS [12,23,24]
						RP-HPLC (MS) [12,24–30]
						CE [31,32]
4 Glycopeptide enrichment	5–8	Tryptic peptides in 50 mM ammonium bicarbonate containing 0.5% RapiGest	Sequential elution of digest from C18 ZipTips or ZipPlate	Enriched glycopeptide fraction in 12% CH_3CN/0.1% TFA	Glycoform heterogeneity and abundance	MALDI-TOF MS [12,33]
						RP-HPLC–MS [27]
						CE [32]

[a] Analyte output serves as sample input for the next process step.
[b] Analytical procedures that can be performed directly on analyte output without further sample processing. References cite examples of techniques employed for MAb characterization. *Abbreviations*: GFC, gel filtration chromatography; NR, non-reducing; IEX, ion-exchange chromatography; CE, capillary electrophoresis; MALDI-TOF MS, matrix-assisted laser desorption/ionization time-of-flight mass spectrometry; RP-HPLC, reverse-phase high performance liquid chromatography.

analytical development process, rapid monitoring of recombinant MAb heterogeneity would enable rational and rapid evaluation of bioprocess unit operations for control of product consistency, assessment of the effect of changes in product structure and pre-screening of producer cells.

In most cases, simple solvent exchange and analyte concentration operations are the most labor-intensive steps, lengthening analytical process time considerably. Here, we describe a generic, microplate-based, high-throughput platform for MAb analyte processing starting from crude cell culture broth. The sample preparation platform can provide analyte for a number of critical quality control analyses within in a single working day (summarized in Table 1). We demonstrate its application to provide quantitative, site-specific analyses of MAb *N*-glycosylation using MALDI-MS.

2. Experimental

All chemicals were of at least analytical quality. All antibody substrates were experimental recombinant humanized IgG2s produced by engineered murine myeloma (NS0) cells in culture supplied by Pfizer Global Biologics, Pfizer Inc.

2.1. Step 1: Affinity purification of rIgG2 MAb using rProtein A

rProtein A Sepharose™ Fast Flow (20 μl bed volume; GE Healthcare, Amersham, UK) was deposited into each well of a MultiScreen Resist-R1 filter plate (Millipore, Billerica, MA). Briefly, rProtein A Sepharose slurry was diluted in an equal volume of 20% (v/v) ethanol and bed volume estimated after centrifugation in a graduated centrifuge tube. The slurry was then diluted to a final concentration of 1:5 in 20% (v/v) ethanol. Well-mixed slurry (100 μl) was then carefully pipetted into each well. To equilibrate the plate prior to use, matrix in each well was washed twice with 200 μl of PBS, removing the liquid phase each time by centrifugation of the microplate for 2 min at 29 × *g* using MultiScreen Centrifuge Align Frames (Millipore) with a polypropylene collection plate in place. Clarified (22 μm filtered) cell culture broth (100 μl) was added to each well and the plate was incubated at 37 °C for 10 min with continuous agitation at 800 rpm using a temperature-controlled orbital shaker (Thermomixer, Eppendorf AG, Hamburg, Germany). The plate was then centrifuged as described above to remove media, and microplate wells rinsed twice with 100 μl PBS to remove unbound contaminants. Adsorbed MAb was eluted directly into

a half-area 96-well UV-transparent microplate (Corning Australia, Sydney, Australia) containing 20 μl of 1 M Tris–HCl, pH 8 per well.

Elution was accomplished by addition of two successive 90 μl aliquots of 50 mM glycine–HCl, pH 2.5 to each well. The first elution step included a 5 min incubation with agitation as described above. rProtein A filterplates were re-equilibrated with PBS containing 0.05% (w/v) sodium azide for long-term storage at 4 °C. Optical density (OD) of the combined eluates at 280 nm was measured with a microplate spectrophotometer (Bio-Tek Instruments, Winooski, VT); antibody mass in each well was calculated with reference to an external calibration based on the OD of equivalent solutions containing defined amounts of purified MAb. Eluted MAb was then transferred to a polypropylene collection plate for storage or transferred to the RPC-microplate (see below) for buffer exchange.

2.2. Step 2: Buffer exchange and in situ reduction/alkylation of affinity purified rIgG2 MAb by reverse-phase chromatography

Source 30RPC (reverse-phase) media (20 μl bed volume; GE Healthcare) diluted 1:5 in 20% (v/v) ethanol, was aliquoted into each well of a 96-well MultiScreen Resist-R1 filterplate as described above, then centrifuged for $29 \times g$ for 2 min to remove the liquid phase. Plates were stored dry or with the resin suspended in 20% (v/v) ethanol with no observable difference in performance. Prior to use resin was first wetted with two successive applications of methanol (200 μl each) followed by equilibration with two 200 μl aliquots of 0.1% (v/v) trifluoroacetic acid (TFA). MAb samples eluted from the rProtein A affinity microplate (in 0.1 M Tris–HCl, 45 mM Gly, pH 8) were transferred to the RPC-microplate which was then agitated at 800 rpm and 37 °C for 10 min. After centrifugation to remove the liquid phase, adsorbed MAb was then washed by two applications of 200 μl 0.1% (v/v) TFA. Desalted whole rIgG2 was then either eluted directly or reduced and alkylated in situ prior to elution. With respect to the latter, 100 μl of reduction/alkylation buffer (RA buffer; 50 mM ammonium bicarbonate, 6 M guanidine–HCl, 3 mM ethylenediaminetetraacetic acid, pH 8) was added to the wells and, after a 3 min incubation at RT, removed by centrifugation. RA buffer (100 μl) containing 50 mM dithiothreitol was then added to each well and the plate agitated at 800 rpm at 37 °C for 60 min. After centrifugation, 100 μl of RA buffer containing 100 mM iodoacetamide was added and the plate agitated as above in the dark for a further 15 min at RT. Wells were then washed three times with 200 μl of 0.1% (v/v) TFA. Whole rIgG2 or reduced and alkylated rIgG2 heavy and light chains were eluted directly into a UV transparent plate (BD Biosciences, San Jose, CA) with three serial additions/centrifugations of 100 μl 50% (v/v) acetonitrile, 0.1% (v/v) TFA at 50 °C. Protein recovery was determined by measurement of OD at 280 nm as described above. For enzymatic digestion, MAb samples were transferred to a polypropylene microplate and dried under vacuum in a SpeedVac™ centrifugal evaporator (ThermoSavant, Holbrook, NY) at 45 °C.

2.3. Step 3: Tryptic digestion of purified, desalted rIgG2

Ammonium bicarbonate buffer (50 μl; 50 mM, pH 8.1) containing RapiGest™ SF acid-labile surfactant (sodium 4-[(2-methyl-2-undecyl-1,3-dioxolan-4-yl) methoxyl]-1-propane sulfonate; Waters, Milford, MA) and 5 μg of sequencing grade trypsin (Sigma, St. Louis, MO) was added to each well. Wells were then sealed with a silicone microplate septum and incubated at 37 °C with agitation at 800 rpm. Digestion was quenched by addition of 10 μl 1% (v/v) TFA to each well.

2.4. Step 4: Fractionation of rIgG2 Fc N-glycopeptides

Peptide fractions enriched in *N*-glycopeptide content were prepared from the tryptic digest of either whole rIgG2 or reduced and alkylated rIgG2 by stepwise elution from C18 ZipTips™ (Millipore). ZipTips were equilibrated with two 10 μl aliquots of 80% (v/v) acetonitrile containing 0.1% (v/v) TFA, followed by two 10 μl aliquots of 0.1% (v/v) TFA. Tryptic digest (5–10 μl) was drawn through the resin five times to maximize binding. ZipTips were then washed with 10 μl of 0.1% (v/v) TFA followed by 10 μl of 7.5% (v/v) acetonitrile, 0.1% (v/v) TFA and eluted directly on to a MALDI target with 1 μl of 12% (v/v) acetonitrile, 0.1% (v/v) TFA.

2.5. MALDI-TOF MS

MALDI-TOF MS was performed with a VOYAGER-DE™ STR instrument (Applied Biosystems, Foster City, CA) in linear (glycopeptide analysis) or reflectron (peptide mapping) positive ion ($[M + H]^+$) mode with delayed extraction. The instrument was externally calibrated with a Proteomass™ peptide calibration kit (Sigma). For both analyses, 1 μl of matrix (50% (v/v) acetonitrile/0.1% (v/v) TFA saturated with α-cyano-4-hydroxy cinnamic acid (CHCA); Sigma) was mixed with an equal volume of sample and allowed to dry on stainless steel target plates at RT.

2.6. Analysis of free N-glycans released from rIgG2 by normal phase HPLC

N-Glycans were released from purified, desalted rIgG2 (100 μg) by peptide-*N*-glycosidase F digestion using an *N*-Glycanase™ kit (Prozyme, San Leandro, CA). The manufacturer's instructions were modified as follows; after addition of the denaturation solution, MAb samples were incubated for 5 min at RT rather than 100 °C, total digestion time was 16–24 h. After protein precipitation with ice-cold ethanol, released *N*-glycans were recovered in the supernatant and dried in a SpeedVac™ centrifugal evaporator. Prior to HPLC analysis, *N*-glycans were then labeled at the reducing terminus with the fluorophore 2-aminobenzamide (2-AB) [34] using a commercially available labeling kit (Prozyme). Labeled *N*-glycans were re-constituted in deionized water. 2-AB labeled *N*-glycans were separated according to hydrodynamic volume by normal-phase HPLC according to the method of Guile et al. [35] using an Agilent 1100 HPLC system (Agilent Technologies, Palo Alto, CA)

equipped with a fluorescence detector (λ_{ex} 330 nm, λ_{em} 420 nm) coupled to a TosoHaas Amide-80 column (4.6 mm × 250 mm, Tosoh Corporation, Tokyo, Japan).

3. Results and discussion

3.1. Step 1: Affinity purification of rIgG2 MAb using rProtein A

We designed a single-pass capture step from cell culture supernatant to be compatible with subsequent direct product assay over the expected range of recombinant MAb concentrations reported for mammalian cell culture [36]. Under the conditions for Protein A based affinity purification of the model rIgG2 employed for this study, recovery of product from the matrix (rProtein A Sepharose Fast Flow beads suspended in each well of a 96-well filter plate, 20 μl bed volume) was essentially complete for product loads in excess of approximately 2 μg (100 μl clarified culture supernatant spiked with rIgG2; Fig. 1A). However, assay of product concentration in eluate by measurement of OD at 280 nm was not reproducible below product loads of approximately 5 μg (Fig. 1B). Above product loads of 25 μg, there was evidence of a slight but progressive decline in product recovery with increased load, although product recovery did not drop below 96% even at a maximum MAb load of 200 μg. MAb purity was confirmed by SDS-PAGE (Fig. 1, inset). We conclude that the conditions employed represent an acceptable compromise between recovery of purified product (96–100%), dynamic range (0.05–2 g rIgG2 per liter) and assay speed (<1 h) and reproducibility (CV < 10%). In our hands micro-affinity plates were re-used at least ten times with no observable decline in performance.

It would be possible to further extend the dynamic range of this primary capture/assay step by increasing either affinity matrix bed volume per well (the absolute MAb binding capacity of the rProtein A Sepharose affinity matrix employed was in significant excess of applied load; approximately 1 mg MAb per well; 20 μl bed volume at approximately 30 mg/ml absolute binding capacity [37]) or product residence time on the affinity matrix. Finally, it is essential to ensure efficient mixing of solid and liquid phases in the microplate format. For example, microplate geometry, the relative density of solid and liquid phases and the diameter and speed of orbital rotation will all affect mixing within the system [38]. One alternative would be the use of Protein A/G affinity membranes for MAb capture [39], however, these materials generally have a much lower absolute binding capacity.

3.2. Step 2: Buffer exchange and in situ reduction/alkylation of affinity purified rIgG2 MAb by reverse-phase chromatography

Purified MAb desorbed from the rProtein A affinity resin in Gly–HCl buffer and neutralized in Tris was rapidly desalted by direct adsorption to Source 30RPC reverse-phase beads (monosized 30 μm polystyrene/divinyl benzene), again suspended in 96-well filter plates. We utilized this procedure to replace more conventional means of buffer exchange prior to protease digestion such as dialysis [18] or gel filtration chromatography [25] as immobilization of the analyte enabled relatively rapid sample processing in the microplate format. This sample preparation step also allows rapid in situ reduction and alkylation (RA) reactions for peptide mapping or other analytical procedures. Although we considered that eluted MAb in 50% (v/v) acetonitrile may be amenable to direct tryptic digestion [40], we

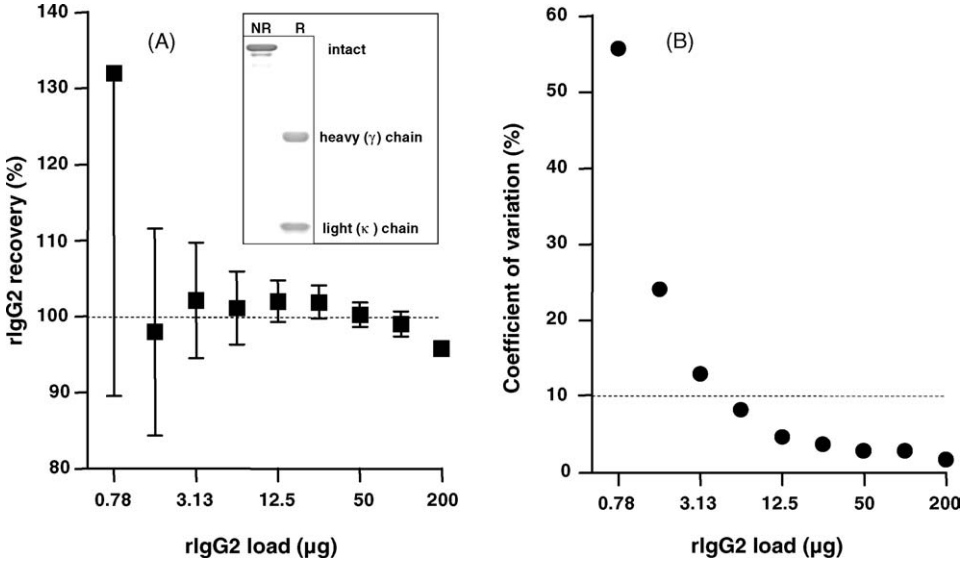

Fig. 1. Step 1: Affinity purification of rIgG2 MAb using rProtein A. Pure rIgG2 was spiked into conditioned mammalian cell culture supernatant at varying concentrations then adsorbed onto rProtein A Sepharose beads suspended in 96-well filterplates for 10 min. After two washes to remove contaminants, purified MAb was eluted directly into UV transparent microplates and optical density at 280 nm was determined. Nine experiments were performed in triplicate. Mean MAb recovery (±S.E.) is shown in (A) and the coefficient of variation in MAb measurement is shown in (B). Inset: MAb purity was confirmed by SDS-PAGE of non-reduced (NR) and reduced (R) rIgG2 MAb (2 μg each) visualized with colloidal Coomassie Blue R250.

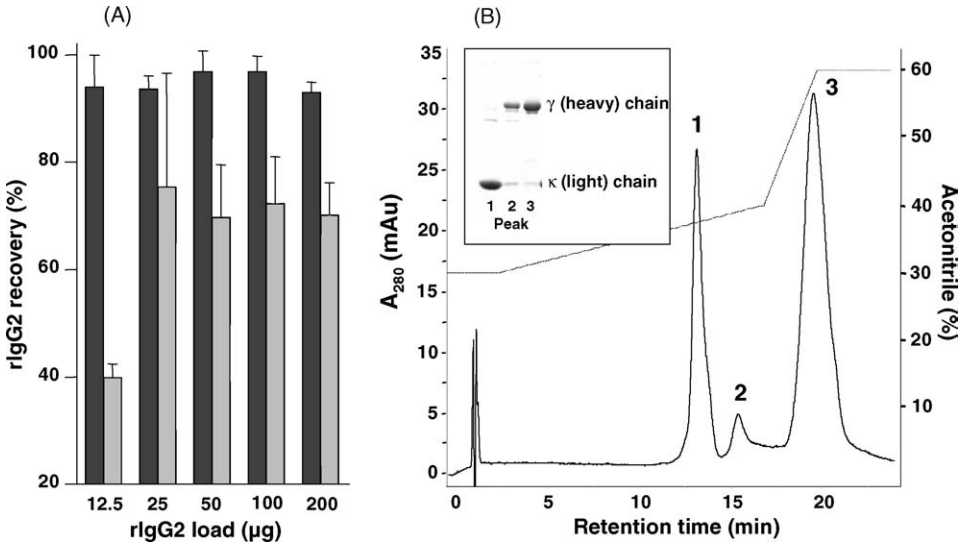

Fig. 2. Step 2: Buffer exchange and in situ reduction/alkylation of affinity purified rIgG2 MAb. rIgG2, purified as described in Fig. 1 was adsorbed onto Source 30RPC beads suspended in 96-well filterplates for 10 min. After two washes to remove salts, bound rIgG2 was then either eluted by centrifugation directly into UV transparent microplates with 50% (v/v) acetonitrile, 0.1% (v/v) TFA or reduced and alkylated in situ with DTT and iodoacetamide prior to elution. Recovery of non-reduced (dark bars) or reduced and alkylated MAb (light bars) is shown in (A) (mean of six replicates ±S.D.). Separation of reduced and alkylated rIgG2 polypeptides (50 μg) by RP-HPLC (Resource RPC 1 ml bed volume; GE Healthcare) using a water/acetonitrile gradient (dotted line) at 1ml/min is shown in (B). Inset: non-reducing SDS-PAGE analysis of major peaks demonstrating separation of γ (heavy; peaks 2, 3) and κ (light; peak 1) chains.

removed volatile organic solvents by centrifugal evaporation to dryness to eliminate variability in sample volume between wells. As described below, MAb samples treated in this way were easily re-dissolved in aqueous tryptic digestion buffer containing RapiGest^{TM} surfactant (Waters).

Sample processing procedures were essentially the same as those described above for the rProtein A affinity plate and were optimized for up to 200 μg rIgG2 binding in a single pass over the adsorbent (we separately determined the absolute binding capacity of Source 30RPC beads to be above 500 μg rIgG2 per 20 μl bed volume deposited in each well). As shown in Fig. 2A, direct recovery of desalted MAb eluted in 50% (v/v) acetonitrile, 0.1% (v/v) TFA without RA was above 93% across a range of MAb loads from 12.5 to 200 μg. However, RA prior to elution decreased MAb recovery by approximately 20%, except at the lowest MAb loading (12.5 μg) where RA reduced recovery to approximately 40%. We speculate that the decrease in MAb recovery after RA is due to decreased binding of MAb polypeptides in the RA buffer containing the denaturant guanidine or, more likely, decreased elution of MAb rendered more hydrophobic after RA.

As human IgG2 has six inter-chain disulfide bonds, we confirmed that the in situ RA procedure yielded free γ (heavy) and κ (light) chains that could be resolved for further analysis, as shown in Fig. 2B. RP-LC of in situ RA MAb yielded the expected single peaks corresponding to γ and κ chains after non-reducing SDS-PAGE analysis, plus a smaller third peak (Fig. 2B, peak 2) which is likely to be non-glycosylated heavy chain (data not shown). To determine the efficiency of the solid-phase RA procedure, we analyzed RA peptides in detail by MALDI-TOF MS after tryptic digestion (as described). Greater than 95% of all cysteine residues were derivatized with iodoacetamide as expected (+57.02 Da; data not shown).

3.3. Step 3: Tryptic digestion of purified, desalted rIgG2

We devised a rapid tryptic digestion protocol that could be employed uniformly across the microplate at varying ratios of protease:substrate. Vacuum dried rIgG2 was re-dissolved in 50 μl of 50 mM ammonium bicarbonate buffer containing 5 μg trypsin, (corresponding to an enzyme:substrate ratio of 1:40 at 200 μg MAb) and an acid-labile surfactant, RapiGest^{TM}, known to promote denaturation and solubilization of substrate proteins without inhibition of trypsin [41,42]. rIgG2 digestion was monitored by MALDI-TOF MS (Fig. 3A), and was optimized with respect to RapiGest^{TM} concentration, MAb load and digestion time. Percent sequence coverage (primary rIgG2 amino acid sequence assigned by MALDI-TOF peptide mapping, comparing observed and expected peptide masses assuming no missed cleavages) was used to compare digestion at varying MAb load (200 μg or 25 μg) and RapiGest^{TM} concentration (0.2% or 0.5%, w/v). As shown in Fig. 3B, tryptic digestion was optimal at relatively low RapiGest^{TM} and MAb concentration, yielding over 80% sequence coverage after just 30 min. Increasing RapiGest^{TM} concentration reduced the rate of MAb digestion efficiency considerably, perhaps mediated by partial denaturation of trypsin. However, at high MAb load (200 μg) this trend was reversed; a higher RapiGest^{TM} concentration promoted tryptic digestion, presumably by more effective denaturation of MAb substrate at the higher load. Overall, our data shows that 0.5% (w/v) RapiGest^{TM} coupled with a 180 min digestion at 37 °C is the most suitable condition for the range of MAb loads we employed. Under these conditions MAb sequence coverage was consistently greater than 85%, for both κ light chain and γ heavy chains. This is comparable to previously published MAb sequence coverage by direct MALDI analysis [23]. However, as we did not include tryptic peptides with a mass below

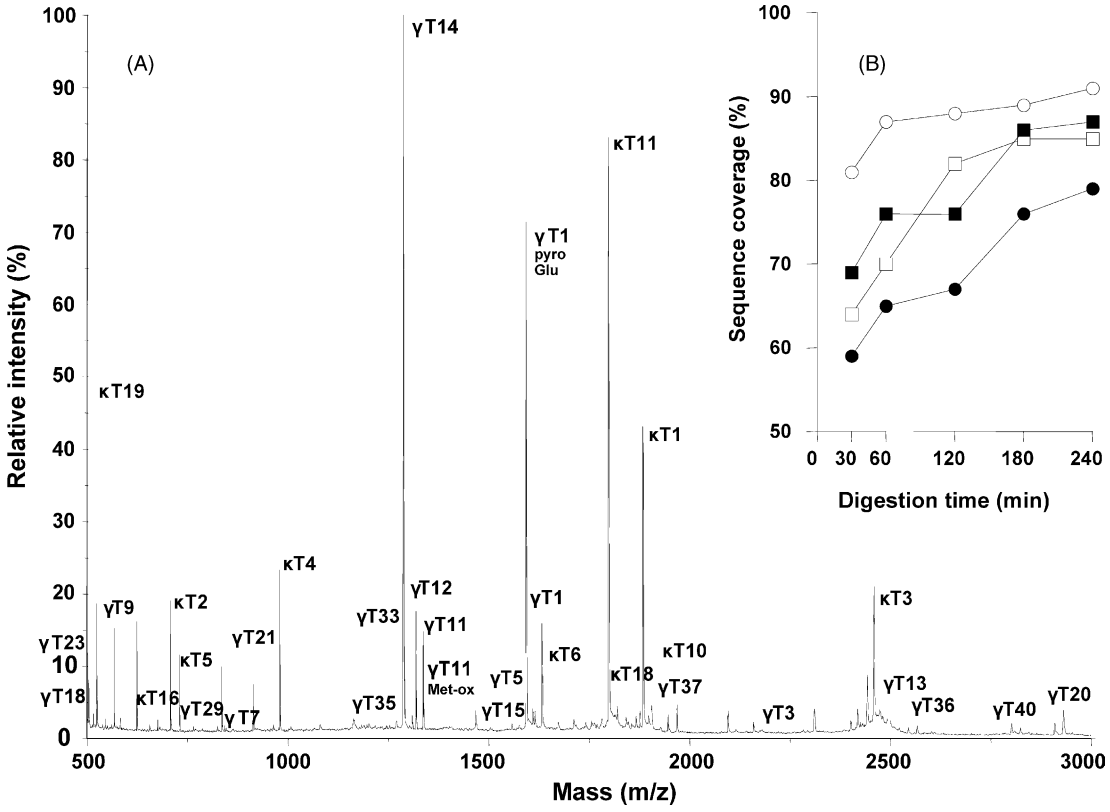

Fig. 3. Step 3: Tryptic digestion of purified, desalted rIgG2. Reduced and alkylated rIgG2 in 50% (v/v) acetonitrile, 0.1% (v/v) TFA derived from in situ buffer exchange (step 2; Fig. 2 was dried in a vacuum centrifuge and re-suspended in 50 μl of 50 mM ammonium bicarbonate containing RapiGest™ surfactant (Waters Corporation, Rydalmere, NSW, Australia) and 5 μg trypsin. Proteolysis at 37 °C was monitored by MALDI-TOF MS. A typical mass spectrum of gamma (heavy) and kappa (light) chain tryptic fragments (deriving from proteolysis of 100 μg rIgG2) identified by comparison of observed and expected masses is shown in (A). As shown in (B), the duration of the digestion process was optimized with respect to rIgG2 load and RapiGest™ concentration. Primary sequence coverage (no missed cleavages) determined by MALDI-TOF MS analysis at 25 μg rIgG2 load (open symbols) and 200 μg rIgG2 load (closed symbols) using either 0.2% (w/v) RapiGest™ (circles) or 0.5% (w/v) RapiGest™ (squares).

500 Da (as MALDI-TOF spectra are obscured by matrix peaks in this mass range), the percent sequence coverage based only on peptides >500 Da was 92% (γ chain) and 94% (κ chain). We note that further identification of peptides having a mass below 500 Da could readily be determined by LC–MS as listed in Table 1.

3.4. Step 4: Fractionation and analysis of rIgG2 Fc N-glycopeptides

N-Glycosylation of recombinant MAbs in the C_H2 domain represents a major source of molecular heterogeneity highly relevant to product bioactivity, particularly for MAbs that utilize on Fc effector functions [2]. To monitor this heterogeneity we developed a rapid procedure for site-specific *N*-glycan analysis based on MALDI-TOF analysis of *N*-glycopeptides derived from the tryptic digestion of rIgG2 in the previous step. As ionization of glycopeptides during MALDI-TOF MS depends upon the peptide moiety [43,44], we compared quantitation of individual glycoforms by this technique with an orthogonal analysis by normal-phase HPLC of fluorophore-labeled *N*-glycans released by PNGaseF.

rIgG2 peptides derived either from tryptic digestion of intact or reduced and alkylated MAb were fractionated by stepwise

Fig. 4. Step 4: Fractionation and analysis of rIgG2 Fc *N*-glycopeptides. Tryptic peptides derived from digestion of non-reduced rIgG2 (performed as described for reduced and alkylated rIgG2 in Fig. 3 in 50 mM ammonium bicarbonate, 0.5% (w/v) RapiGest™ were concentrated and selectively fractionated by immobilization on reverse-phase C18 ZipTips™ followed by stepwise elution in 0.1% (v/v) TFA at increasing acetonitrile concentration. The γ (heavy) chain Fc glycopeptide (EEQFNSTFR, average mass 1157.21 Da) heterogeneously modified with *N*-glycans at Asn294 was eluted by a step change in acetonitrile concentration from 7.5% to 12% (v/v). Eluted glycopeptides (1 μl) were deposited directly on the MALDI target surface and mixed with CHCA matrix (1 μl). Direct analysis of rIgG2 the Fc glycopeptide by MALDI-TOF MS in linear, positive ion mode ($[M+H]^+$ molecular ions) is shown in (A). To identify discrete glycoforms, the core (singly protonated) tryptic glycopeptide mass (1158.21 Da) was subtracted from the average mass of observed peptide species to yield potential *N*-glycan masses (listed in C). Calculated *N*-glycan masses that conformed to a monosaccharide composition and were used to infer an *N*-glycan structure consistent with mammalian biosynthetic principles [45]. Monosaccharides are represented as follows: (■) *N*-acetyl glucosamine, (●) mannose, (▲) galactose, (⋆) fucose. A comparative NP-HPLC analysis of free *N*-glycans released from rIgG2 by PNGaseF and derivatized at the reducing terminus with 2-aminobenzamide is shown in (B). *N*-glycan structures were deduced by comparison of hydrodynamic volumes [35] and separate MS analyses coupled with exoglycosidase array sequencing (data not shown).

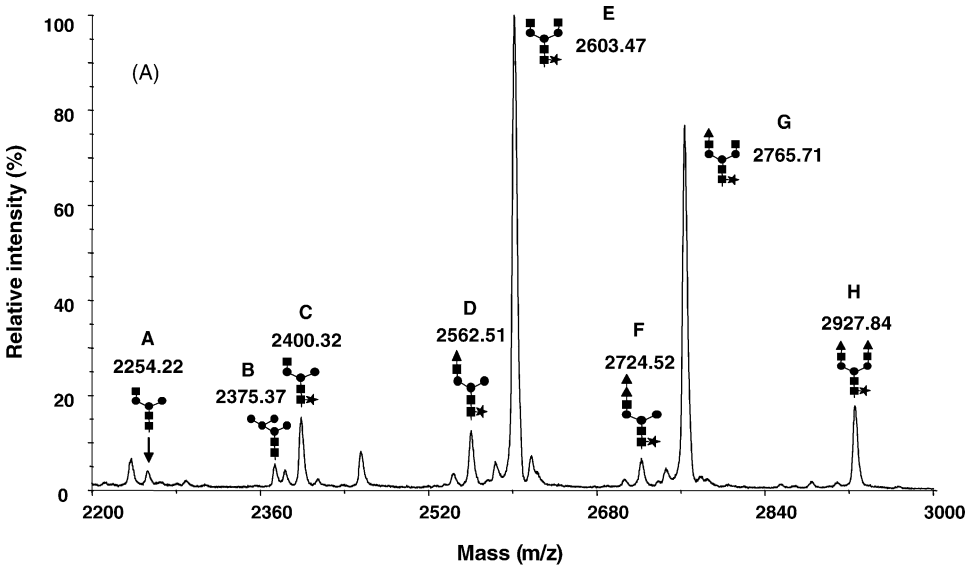

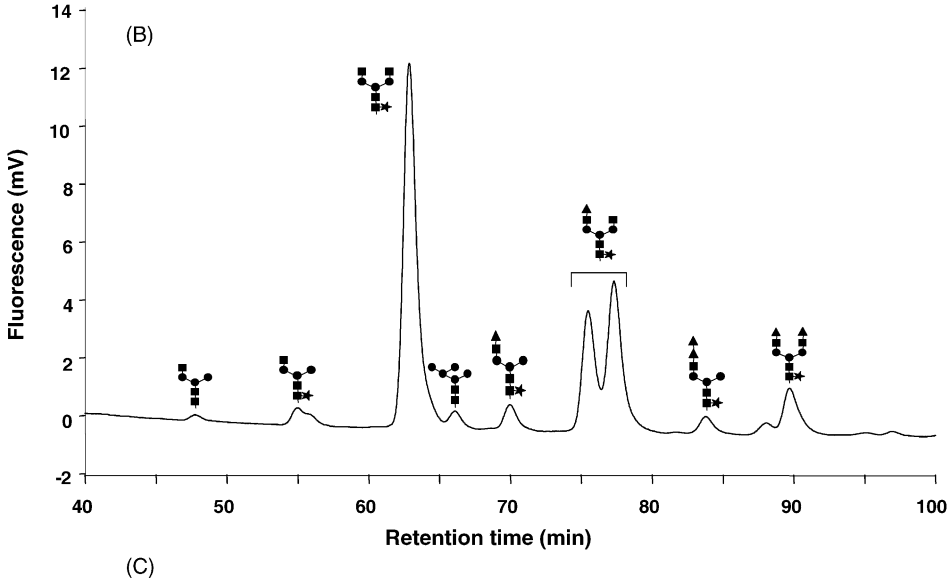

(C)

Peak	Observed glycopeptide mass ([M+H]+, Da)	Corresponding N-glycan mass (Da)	Monosaccharide composition	Proposed oligosaccharide structure
A	2254.22	1096.01	$HexNAc_3Hex_3$	A1G0
B	2375.37	1217.10	$HexNAc_2Hex_5$	MAN5
C	2400.32	1242.16	$Deoxyhex_1HexNAc_3Hex_3$	A1G0F
D	2562.51	1404.30	$Deoxyhex_1HexNAc_3Hex_4$	A1G1F
E	2603.47	1445.35	$Deoxyhex_1HexNAc_4Hex_3$	A2G0F
F	2724.52	1566.44	$Deoxyhex_1HexNAc_3Hex_5$	A1G2F
G	2765.71	1607.49	$Deoxyhex_1HexNAc_4Hex_4$	A2G1F
H	2927.84	1769.63	$Deoxyhex_1HexNAc_4Hex_5$	A2G2F

elution from C18 reverse-phase pipet tips (ZipTips™, Millipore), directly onto a MALDI-TOF MS target for analysis. Using this approach, rIgG2 Fc *N*-glycopeptides (core peptide EEQFNSTFR, varying in *N*-glycan composition at Asn294) were found to co-elute on a step change in acetonitrile concentration from 7.5% to 12% (v/v). Direct MALDI-TOF MS analysis (Fig. 4A) revealed that this fraction largely comprised the *N*-glycopeptide pool. After subtraction of the core peptide mass (1157.21 Da) from observed peptides, residual masses that allowed calculation of a monosaccharide composition that conformed to known mammalian biosynthetic pathways (i.e. presence of a trimannosyl chitobiose core [45]) were assigned the appropriate *N*-glycan structure (Fig. 4C). Eight possible *N*-glycan structures accounted for the vast majority of signal observed within a mass range of 2200–3000 Da (as $[M+H]^+$ ions). These structures were also in accord with previous analyses of Fc *N*-glycans associated with recombinant MAbs produced by engineered myeloma cells [5,10,33]. The major glycoforms were variably galactosylated, core fucosylated biantennary structures (peaks E, G, H in Fig. 4A), as well as smaller proportions of either incompletely processed (e.g. high-mannose, peak B) or *N*-glycans having one antenna apparently truncated to the core trimannosyl α-mannose (peaks A, C, D, F). We identified one glycoform (peak F) as having a terminal α1–3 Gal residue on one antenna, which is typical of glycoproteins produced by murine myeloma cells [46,47]. In order to demonstrate that the *N*-glycoform profile observed by MALDI-TOF MS was comparable to that observed by a different analytical procedure, we analyzed oligosaccharides released from rIgG2 with PNGaseF by normal-phase HPLC as described previously [35,47]. A typical separation of fluorophore-labeled oligosaccharides is shown in Fig. 4B. The eight glycans detected by MALDI-TOF MS of rIgG2 glycopeptides were also observed by NP-HPLC, and their identity separately confirmed by MALDI-TOF MS and exoglycosidase array sequencing (data not shown).

To validate the use of MALDI-TOF MS as a tool to quantitate the relative abundance of rIgG2 *N*-glycoforms, we compared glycopeptide analysis based on the high-throughput platform described with NP-HPLC analysis of released, fluorophore labeled *N*-glycans. Four discrete rIgG2 MAbs with different glycosylation profiles were each analyzed, and examples of MALDI-TOF MS glycopeptide spectra are shown in Fig. 5A. In each case, mean mass spectral peak heights were employed to calculate the relative abundance of the eight individual glycoforms identified as a percent of total (Fig. 5B). Relative glycoform abundances determined by MALDI-TOF MS were then compared with the relative abundance of the corresponding glycoforms determined by NP-HPLC. The derived ratio (MALDI-TOF MS/NP-HPLC) for each glycoform is also shown in Fig. 5B. Therefore, assuming that the NP-HPLC analysis accurately measures the absolute abundance of each glycoform, ratios greater than one indicate an overestimation of glycoform abundance by MALDI-TOF MS. For the major variably galactosylated rIgG2 glycoforms typically associated with MAbs (Fig. 5, peaks E, G, H), determination of their relative abundance by both techniques was approximately equivalent. This was also the case for the incompletely processed high-mannose *N*-glycan (MAN5, peak B). However, truncated glycoforms with a terminal core trimannosyl α-mannose (i.e. lacking one antenna, peaks A, C, D, F) were generally overestimated by MALDI-TOF MS (MALDI/NPLC ratio > 1.5) where the abundance of that glycoform estimated by MALDI was relatively low (<5–9%). This was not the case for non-truncated *N*-glycans in low abundance (e.g. peaks B, H). These data suggest that the MALDI process itself contributes to the appearance of truncated glycoforms with a free α-mannose by fragmentation of more abundant ions. As reported by Naven et al., fragment ions arising by in-source decay of glycosidic bonds may be observed by MALDI-TOF in linear mode where the MALDI instrument is fitted with delayed extraction (temporary retention of ions in the ion source) to improve resolution [48]. Furthermore, preferential loss of the antenna attached to the C-3 of the core β-mannose via cleavage of the glycosidic bond linking the non-reducing GlcNAc is possible [49,50]. We suggest therefore that it is highly likely that in-source fragmentation of abundant glycopeptides (e.g. glycoforms E and G yielding glycoforms C and D) contributes to their overestimation by MALDI. However, this does not wholly explain the presence of truncated glycoforms also observable by NP-HPLC that could not arise biosynthetically. We suggest that another mechanism, such as extracellular digestion of *N*-glycans in culture broth by glycosidases released by dead cells is a likely cause [51].

Finally, we examined the relationship between glycoform abundance and variability in measurement by MALDI-TOF MS, and specifically the extent to which variability in measurement of low abundance glycopeptides is related to in-source decay during glycopeptide analysis by MALDI. As shown in Fig. 6, for measured relative glycoform abundances below 5% (18/32 measurements), 39% of these (7/18) had coefficients of variation (CV) in excess of 10%. Importantly, there was no distinction between truncated (Fig. 4, glycoforms A, C, D, F) and non-truncated (glycoforms B, E, G, H) species with respect to CV. Therefore, MALDI-TOF MS of glycopeptides is quantitatively precise at relative glycopeptide abundances above 5%. With respect to the accuracy of determination of glycopeptide abundance by MALDI-TOF MS, the mean MALDI/NPLC ratio for non-truncated glycans (above 5% relative abundance by MALDI analysis) was 0.98 with a standard deviation of 0.18. Therefore, for non-truncated glycans, MALDI/NPLC ratios greater than 1.55 (mean ± 3 S.D.) occur at $p < 0.01$. Truncated glycans, which tend to be overestimated by MALDI, exceeded this MALDI/NPLC ratio of 1.55 at estimated relative abundances of approximately 7% or less. We conclude that *N*-glycoform analysis by MALDI-TOF MS of glycopeptides using this approach is quantitatively reliable at measured relative glycoform abundances greater than 5–7%. We note that for these MALDI-TOF MS assays of glycopeptide abundance we took no specific steps to control crystal formation on the target surface to reduce analyte-matrix heterogeneity. Sample preparation techniques such as the fast evaporation method to generate a uniform thin crystal layer [52] may result in quantitative MALDI analyses with improved precision.

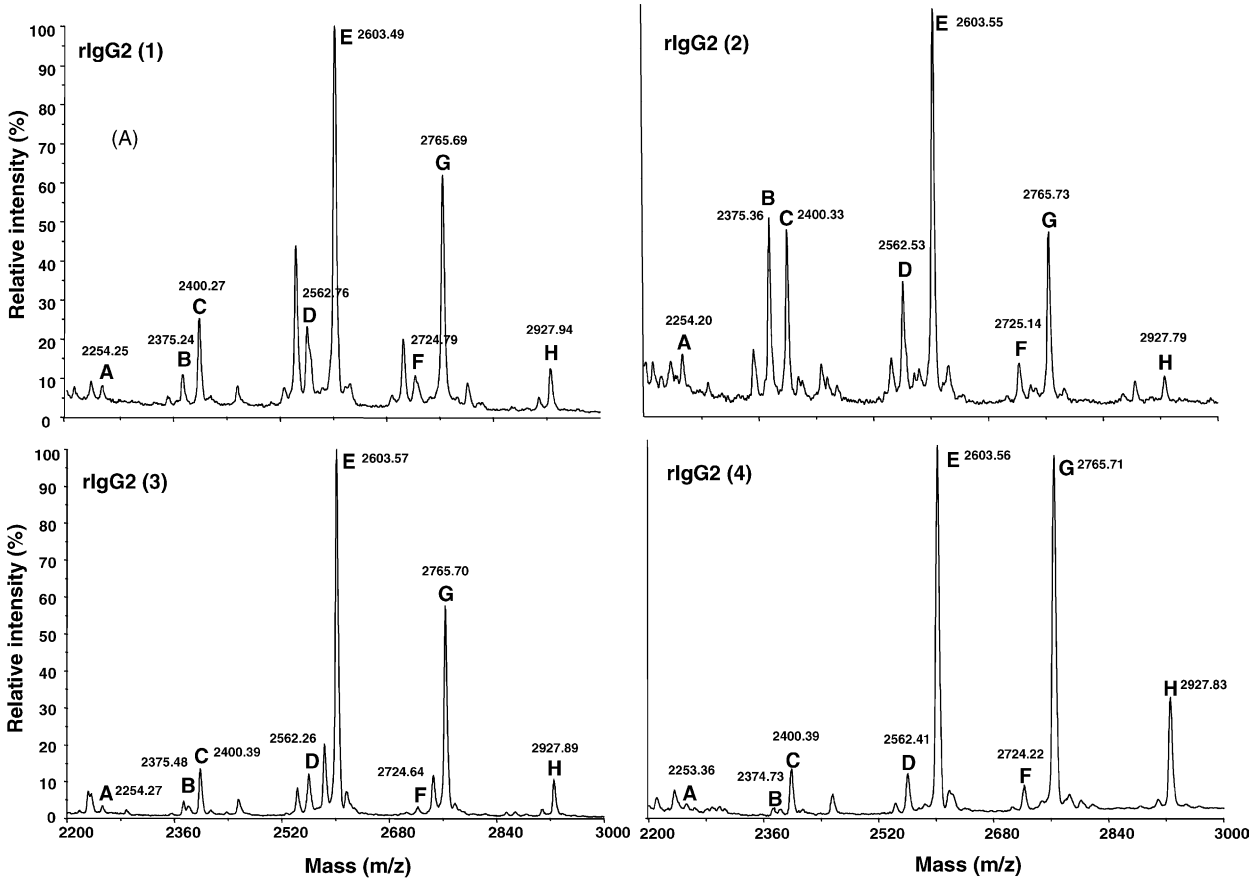

(B)

Peak	MALDI-MS relative glycoform abundance (% of total) rIgG2				MALDI/NPLC ratio rIgG2			
	1	2	3	4	1	2	3	4
A	3.6	5.7	1.9	1.6	4.2	3.1	6.5	16.2
B	4.5	16.7	2.2	1.1	1.0	0.9	1.1	1.2
C	10.1	16.0	6.5	5.1	1.1	1.2	1.9	4.0
D	9.2	10.7	6.4	4.4	1.2	1.2	3.9	2.0
E	38.7	32.1	49.0	37.6	0.8	0.9	0.9	1.0
F	4.6	3.8	1.5	2.3	1.2	2.6	3.5	1.1
G	23.8	12.8	27.5	36.7	1.0	0.7	1.0	0.9
H	5.2	2.2	5.0	11.3	1.4	0.8	1.3	0.9

Fig. 5. Comparative quantitation of rIgG2 glycoform abundance by MALDI-TOF MS and NP-HPLC of released *N*-glycans. For four discrete rIgG2 MAbs, *N*-glycans at Asn294 were analyzed by both MALDI-TOF MS of glycopeptides using the microplate-based sample processing method described and by NP-HPLC of 2-aminobenzamide labeled *N*-glycans released by PNGaseF. Representative MALDI-TOF spectra are shown in (A), with individual glycoforms identified as described in Fig. 4. In each case, $[M+H]^+$ peak heights were employed to determine the relative abundance of individual glycoforms as a percent of total. These data are shown in (B) for each rIgG2 MAb (each number is mean of four replicate analyses). Each rIgG2 was also analyzed by NP-HPLC. In this case, peak areas were used to quantitate relative glycoform abundance (data not shown). Corresponding MALDI-TOF MS and NP-HPLC data are expressed as a ratio to compare quantitation of individual *N*-glycans by both methods.

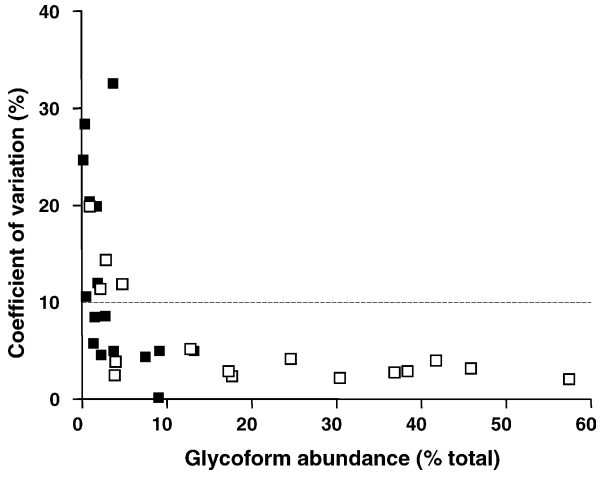

Fig. 6. Variation in measurement of glycoform abundance by MALDI-TOF MS of glycopeptides. The relationship between glycoform abundance and variability in quantitation by MALDI-TOF MS was examined by calculation of the coefficient of variation (%) in measurement of relative glycoform abundance (as percent of total). For each of the four discrete rIgG2 proteins, the glycopeptide analysis by MALDI-TOF MS was repeated four times, each time measuring the relative abundance of the eight distinct glycoforms (i.e. a total of 32 determinations of CV). Open squares, non-truncated glycoforms (B, E, G, H in Fig. 4); closed squares, truncated glycoforms (A, C, D, F in Fig. 4).

4. Conclusion

In this study, we describe a microplate-based sample preparation platform for rapid, high-throughput monoclonal antibody quantitation and analysis. This strategy effectively bridges the interface between the analyte processing stream and a variety of analytical technologies using high-capacity adsorbents to exchange solvents rapidly whilst maintaining analyte concentration. The platform was designed to utilize concentrations of analyte that are both relevant to volumetric concentrations of MAb typical of mammalian cell culture (0–2 g/L) and to yield analyte mass necessary for typical LC or MS-based analyses. We aimed for as simple and robust a procedure as possible, where handling of multiple samples at varying concentration within a defined range could occur simultaneously.

We believe this sample preparation strategy would find utility in various aspects of recombinant MAb product development; from cell clone selection to product formulation and long-term stability studies. As each stage of product development may require different analytical outcomes, the platform can be easily adapted. For example, MAb reduction and alkylation may be omitted to expedite preparation of glycopeptides. Additional analyte processing steps may also be added to generate more detailed information. For example, detailed structural characterization of glycopeptide-associated oligosaccharides can be carried out relatively rapidly using sequential exoglycosidase arrays with MALDI-TOF MS [43,44], potentially facilitated either by on-target digestion [53] or enzymes linked to paramagnetic beads [54].

We considered that any sample preparation platform should ideally be amenable for automation. This could be achieved simply by replacement of the solid phase adsorbents we employed with magnetized beads derivatized with similar functional groups. This would enable effective phase-separations based on a simple pipet on/pipet off approach. Moreover, direct interface of a sample-handling robot with an automated analytical device (such as a HPLC autosampler) is eminently feasible.

Acknowledgement

M.J.B. gratefully acknowledges funding for a postdoctoral fellowship from Pfizer Central Research.

References

[1] US Department of Health and Human Services–Food and Drug Administration (1999) Guidance for industry, Q6B specifications: test procedures and acceptance criteria for biotechnological/biological products (http://www.fda.gov/cder/guidance/Q6Bfnl.PDF).
[2] R. Jefferis, Biopharm 14 (2001) 19.
[3] A. Wright, S.L. Morrison, Trends Biotechnol. 15 (1997) 26.
[4] D.M. Sheeley, B.M. Merrill, L.C. Taylor, Anal. Biochem. 247 (1997) 102.
[5] M.R. Lifely, C. Hale, S. Boyce, M.J. Keen, J. Phillips, Glycobiology 5 (1995) 813.
[6] D.K. Robinson, C.P. Chan, C. Yu Ip, P.K. Tsai, J. Tung, T.C. Seamans, A.B. Lenny, D.K. Lee, J. Irwin, M. Silberklang, Biotechnol. Bioeng. 44 (1994) 727.
[7] S.B. Mohan, S.R. Chohan, J. Eade, A. Lyddiatt, Biotechnol. Bioeng. 42 (1993) 974.
[8] M. Marino, A. Corti, A. Ippolito, G. Cassani, G. Fassina, Biotechnol. Bioeng. 54 (1997) 17.
[9] J.P. Kunkel, D.C. Jan, M. Butler, J.C. Jamieson, Biotechnol. Prog. 16 (2000) 462.
[10] A.E. Hills, A. Patel, P. Boyd, D.C. James, Biotechnol. Bioeng. 75 (2001) 239.
[11] T.P. Patel, R.B. Parekh, B.J. Moellering, C.P. Prior, Biochem. J. 285 (1992) 839.
[12] G.D. Roberts, W.P. Johnson, S. Burman, K.R. Anumula, S.A. Carr, Anal. Chem. 67 (1995) 3613.
[13] D.I. Papac, J.B. Briggs, E.T. Chin, A.J.S. Jones, Glycobiology 8 (1998) 445.
[14] L. Li, M. Sun, Q.S. Gao, S. Paul, Mol. Immunol. 33 (1996) 593.
[15] L. Deng, D. Wylie, Y.S. Tsao, B. Larkin, M. Voloch, W.L. Ling, Biotechnol. Appl. Biochem. 40 (2004) 261.
[16] K. Forrer, S. Hammer, B. Helk, Anal. Biochem. 334 (2004) 81.
[17] W. Zhang, M.J. Czupryn, Biotechnol. Prog. 18 (2002) 509.
[18] R.J. Harris, B. Kabakoff, F.D. Macchi, F.J. Shen, M. Kwong, J.D. Andya, S.J. Shire, N. Bjork, K. Totpal, A.B. Chen, J. Chromatogr. B 752 (2001) 233.
[19] W. Zhang, M.J. Czupryn, J. Pharm. Biomed. Anal. 30 (2003) 1479.
[20] M. Perkins, R. Theiler, S. Lunte, M. Jeschke, Pharm. Res. 17 (2000) 1110.
[21] G. Hunt, W. Nashabeh, Anal. Chem. 71 (1999) 2390.
[22] G. Hunt, K.G. Moorhouse, A.B. Chen, J. Chromatogr. A 744 (1996) 295.
[23] L.E.M. Fernandez, D.E. Kalume, L. Calvo, M. Fernandez Mallo, A. Vallin, P. Roepstorff, J. Chromatogr. B 752 (2001) 247.
[24] R. Mhatre, J. Woodard, C. Zeng, Rapid Commun. Mass Spectrom. 13 (1999) 2503.
[25] J. Bongers, J.J. Cummings, M.B. Ebert, M.M. Federici, L. Gledhill, D. Gulati, G.M. Hilliard, B.H. Jones, K.R. Lee, J. Mozdzanowski, M. Naimoli, S. Burman, J. Pharm. Biomed. Anal. 21 (2000) 1099.
[26] K. Kannan, M.G. Mulkerrin, M. Zhang, R. Gray, T. Steinharter, K. Sewerin, R. Baffi, R. Harris, C. Karunatilake, J. Pharm. Biomed. Anal. 16 (1997) 631.
[27] K. Hirayama, R. Yuji, N. Yamada, K. Kato, Y. Arata, I. Shimada, Anal. Chem. 70 (1998) 2718.

[28] J.W. Bloom, M.S. Madanat, D. Marriott, T. Wong, S.Y. Chan, Protein Sci. 6 (1997) 407.
[29] W. Zhang, L.A. Marzilli, J.C. Rouse, M.J. Czupryn, Anal. Biochem. 311 (2002) 1.
[30] D.A. Lewis, A.W. Guzzetta, W.S. Hancock, M. Costello, Anal. Chem. 66 (1994) 585.
[31] N. Bihoreau, C. Ramon, R. Vincentelli, J.P. Levillain, F. Troalen, J. Capillary Electrophor. 2 (1995) 197.
[32] N. Bihoreau, C. Ramon, M. Lazard, J.M. Schmitter, J. Chromatogr. B 697 (1997) 123.
[33] D.J. Kroon, J. Freedy, D.J. Burinsky, B. Sharma, J. Pharm. Biomed. Anal. 13 (1995) 1049.
[34] J.C. Bigge, T.P. Patel, J.A. Bruce, P.N. Goulding, S.M. Charles, R.B. Parekh, Anal. Biochem. 230 (1995) 229.
[35] G.R. Guile, P.M. Rudd, D.R. Wing, S.B. Prime, R.A. Dwek, Anal. Biochem. 240 (1996) 210.
[36] W.C. Zhou, C.C. Chen, B. Buckland, J. Aunins, Biotechnol. Bioeng. 55 (1997) 783.
[37] R. Hahn, R. Schlegel, A. Jungbauer, J. Chromatogr. B 790 (2003) 35.
[38] S. Weiss, G.T. John, I. Klimant, E. Heinzle, Biotechnol. Prog. 18 (2002) 821.
[39] O.P. Dancette, J.L. Taboureau, E. Tournier, C. Charcosset, P. Blond, J. Chromatogr. B 723 (1999) 61.
[40] L.M. Simon, M. Kotorman, G. Garab, I. Laczko, Biochem. Biophys. Res. Commun. 280 (2001) 1367.
[41] P. Suder, A. Bierczynska, S. Konig, J. Silberring, Rapid Commun. Mass Spectrom. 18 (2004) 822.
[42] Y.Q. Yu, M. Gilar, P.J. Lee, E.S. Bouvier, J.C. Gebler, Anal. Chem. 75 (2003) 6023.
[43] C.W. Sutton, J.A. O'Neill, J.S. Cottrell, Anal. Biochem. 218 (1994) 34.
[44] D.C. James, R.B. Freedman, M. Hoare, O.W. Ogonah, B.C. Rooney, O.A. Larionov, V.N. Dobrovolsky, O.V. Lagutin, N. Jenkins, Bio-Technology 13 (1995) 592.
[45] H. Schachter, Biochem. Cell Biol. 64 (1986) 163.
[46] N. Jenkins, R.B. Parekh, D.C. James, Nat. Biotechnol. 14 (1996) 975.
[47] K.N. Baker, M.H. Rendall, A.E. Hills, M. Hoare, R.B. Freedman, D.C. James, Biotechnol. Bioeng. 73 (2001) 188.
[48] T.J.P. Naven, D.J. Harvey, J. Brown, G. Critchley, Rapid Commun. Mass Spectrom. 11 (1997) 1681.
[49] D.J. Harvey, Mass Spectrom. Rev. 18 (1999) 349.
[50] D.J. Harvey, B. Kuster, T.J. Naven, Glycoconj. J. 15 (1998) 333.
[51] M.J. Gramer, C.F. Goochee, Biotechnol. Bioeng. 43 (1994) 423.
[52] O. Vorm, P. Roepstorff, M. Mann, Anal. Chem. 66 (1994) 3281.
[53] H. Geyer, S. Schmitt, M. Wuhrer, R. Geyer, Anal. Chem. 71 (1999) 476.
[54] T.N. Krogh, T. Berg, P. Hojrup, Anal. Biochem. 274 (1999) 153.